Distributed Motion Control for Multiple Mobile Robots Using Discrete-Event Systems and Model Predictive Control

Yuan Zhou, *Member, IEEE*, Hesuan Hu, *Senior Member, IEEE*, Gelei Deng, Kun Cheng, Shang-Wei Lin, Yang Liu, *Senior Member, IEEE*, and Zuohua Ding

***Abstract*—Distributed motion control is critical in multiple mobile robot systems (MMRSs). Current research usually focuses on either discrete approaches, which aim to deal with high-level collisions and deadlocks without considering the low-level motion commands, or continuous approaches, which can optimize low-level continuous commands to mobile robots but cannot deal with deadlocks efficiently. In this article, by combining discrete and continuous methods, we design a hybrid motion control method for MMRSs where each robot should move along a predefined path. First, each robot's motion is modeled as a discrete transition system, based on which a real-time supervisory control policy is illustrated to avoid collisions and deadlocks. Second, according to the discrete decisions, the continuous speed at each discrete state is computed using model predictive control and sequential convex programming. The proposed hybrid approach brings two advantages. First, the discrete control component guarantees collision and deadlock avoidance and reduces the scale of the optimization problems. Second, continuous control optimizes the continuous speed in real time and fulfills other performance requirements like time and energy costs. To move in a fully distributed way, each robot needs to predict the motion of its neighbors by retrieving their immediately available information through communications. The simulation and real-world experimental results show the effectiveness of our approach.**

***Index Terms*—Collision and deadlock avoidance, hybrid control, motion planning, multiple mobile robot systems (MMRSs).**

I. Introduction

A MULTIPLE mobile robot system (MMRS) is a system where multiple mobile robots work together to finish given tasks by moving around in a given environment. MMRSs exhibit many advantages, such as increasing spatial coverage and temporal throughput [1] and dramatic capability to resolve task complexity and efficiency [2]. They have been well studied and applied in many fields [2], [3]. Motion planning is one of the most critical tasks in MMRSs, and different approaches have been proposed, which usually focus on unstructured environments [4], [5], [6], [7], [8].

However, in some scenarios, such as intelligent transportation systems, smart warehouses, and environmental surveillance, robots move in structured environments, i.e., the paths of robots are determined in advance and cannot be changed. For example, autonomous vehicles are required to move along particular roads because of infrastructure limitations; in multirobot cooperative patrolling, each robot is required to track a set of objects [9], [10], [11]. In such scenarios, motion planning is to compute a collision-free velocity profile for each robot. Even though off-line methods can be applied to compute velocity profiles for robots in advance, such methods not only require all the information in the system to be predictable, accurate, and determined but also will compromise the performance and flexibility of the system. While real-time continuous motion planning methods, such as model predictive control (MPC) methods [12], can be applied, deadlocks may arise. Hence, real-time and distributed motion planning methods are investigated for such systems [13], [14], [15], [16]. Soltero et al. [13] and Liu et al. [14] investigated collision avoidance and decision deadlock avoidance in such a system by computing a proper speed for each robot; however, physical deadlocks are not considered. In [15] and [16], we consider deadlock and higher-order deadlock avoidance in terms of discrete-event control by neglecting the control of continuous velocity. They do not consider the low-level continuous motion control.

Herein, integrating the advantages of discrete and continuous approaches, we develop a real-time, distributed, and hybrid

Manuscript received 26 January 2023; revised 14 June 2023; accepted 28 September 2023. Date of publication 24 October 2023; date of current version 17 January 2024. This work was supported in part by the Ministry of Education, Singapore, under its Academic Research Fund (AcRF) Tier 2 under Grant MOE-T2EP20120-0004; in part by the National Research Foundation, Singapore, and DSO National Laboratories through the AI Singapore Programme (AISG) under Award AISG2-GC-2023-008; in part by the NRF Investigatorship under Grant NRF-NRFI06-2020-0001; in part by the Natural Science Foundation of China under Grant 61973242, Grant 61573265, Grant 61203037, and Grant 62132014; in part by the New Century Excellent Talents in University under Grant NCET-12-0921; in part by the Major Fundamental Research Program of the Natural Science Foundation of Shaanxi Province under Grant 2017ZDJC-34; and in part by the Zhejiang Provincial Key Research and Development Program of China under Grant 2022C01045. This article was recommended by Associate Editor C. Yang. *(Corresponding author: Hesuan Hu.)*

Yuan Zhou, Gelei Deng, Shang-Wei Lin, and Yang Liu are with the School of Computer Science and Engineering, Nanyang Technological University, Singapore 639798 (e-mail: y.zhou@ntu.edu.sg; gelei.deng@ntu.edu.sg; shang-wei.lin@ntu.edu.sg; yangliu@ntu.edu.sg).

Hesuan Hu is with the School of Electro-Mechanical Engineering, Xidian University, Xi'an 710071, Shaanxi, China (e-mail: hshu@mail.xidian.edu.cn).

Kun Cheng is with the State Key Laboratory of Software Development Environment, Beihang University, Beijing 100191, China (e-mail: chengkun@buaa.edu.cn).

Zuohua Ding is with the School of Computer Science and Technology, Zhejiang Sci-Tech University, Hangzhou 310018, Zhejiang, China (e-mail: zuohuading@zstu.edu.cn).

This article has supplementary material provided by the authors and color versions of one or more figures available at https://doi.org/10.1109/TSMC.2023.3322154.

Digital Object Identifier 10.1109/TSMC.2023.3322154

motion planning method, combining discrete-event systems and MPC, for robots moving along their predefined and closed paths persistently. By modeling the motion of each robot as a discrete transition system, the method first designs an online supervisory control policy to predict whether the firing of its current transition would cause collisions or deadlocks. Then, a continuous control strategy is designed to adjust the motion speed via MPC. One of the key difficulties in this combination lies in coordinating the two methods effectively. Specifically, we need to determine how to translate discrete decisions (i.e., deciding whether the current transition can be fired) into constraints for the optimization problem within the MPC framework. To tackle this challenge, we propose a distributed method that predicts the waiting time of a robot based on the discrete decisions. Subsequently, an optimization problem is formulated by incorporating the motion time constraint, ensuring that the actual motion time exceeds the predicted waiting time. By leveraging the time constraint, these two methods are effectively coordinated to generate a smooth motion without causing any deadlock or collision. This method can generate optimal speeds for robots such that each one can move to its next state as smoothly as possible. To move in a fully distributed manner, each robot needs to communicate with its neighbors to retrieve their current status for motion prediction. The main contributions of this work are as follows.

1) A hybrid and fully distributed approach is proposed for MMRSs where each robot has a predefined path. It consists of a discrete transition control policy for collision and deadlock avoidance and an MPC-based continuous control module for speed optimization.
2) A small and fixed-scale optimization problem is built at each horizon of MPC, being independent of the number of robots in the system. It aims to increase computational efficiency and motion stability.

II. Related Work

Motion planning is one of the essential issues in MMRSs, which aims to plan a collision-free motion for each robot. In the past decades, robot motion planning has received considerable attention, deriving various methods [4], [5], [6], [7], [8], [12], [17], [18], [19], [20], [21], [22], [23], [24]. They can be roughly divided into discrete and continuous methods.

Usually, discrete methods first discretize the motion space into a set of discrete regions or points and then find a feasible path among them to satisfy some requirements using graph search algorithms, such as A* and D*. Some typical discrete methods are formal methods [4], [25], cell decomposition [5], state lattices [6], [26], roadmap methods [7], [17], and incremental sampling-based methods [8], [18]. Discrete methods can simplify motion control; however, they do not explicitly consider the kinematics or dynamics of robots and thus cannot provide low-level continuous control commands, e.g., acceleration or speed, to robots' actuators.

Continuous methods, such as bug-based algorithms [19], potential field-based methods [20], [21], reciprocal velocity obstacles [22], and mathematical programming [12], [23], [24], regard the environment as a continuous Euclidean space and consider the kinematics and/or dynamics of robots. They can generate low-level continuous control inputs to actuators directly. For example, mathematical programming methods consider different constraints, such as mechanism and collision avoidance constraints, and objectives (e.g., motion time and control efforts) to build optimization problems [27]. The optimization problems are usually resolved approximately via convex programming [12], [23]. However, for complex environments or a large number of robots, continuous methods usually cause high computation costs, and they are incapable of dealing with deadlocks.

To leverage their advantages and mitigate their limitations, we propose a hybrid motion planning method for robots performing persistent motion along predefined paths. It combines discrete transition systems and MPC.

III. Problem Statement

Suppose that there are n mobile robots, $\{r_i : i = 1, 2, \ldots, n\}$, in an MMRS, and each robot r_i has a predefined path P^i. It is a directed curve defined by a parameter equation: $P^i = P^i(\theta)$, $\theta \in [0, 1]$, where $P^i(\theta)$ is a continuously differentiable function mapping from $[0, 1]$ to the 2-D or 3-D space. $d(x, y) = \|x - y\|_2$ denotes the Euclidean distance between the two points x and y. Given the kth path segment $P^i_k = \{P^i(\theta) : \theta_1 \leq \theta \leq \theta_2\}$, the distance between x and P^i_k, denoted as $d(x, P^i_k)$, can be described as $d(x, P^i_k) = \inf_{y \in P^i_k} d(x, y)$.

Definition 1: Given a path $P^i(\theta)$, $p_1 = P^i(\theta_1)$ and $p_2 = P^i(\theta_2)$ are two arbitrary points on it. The path length from p_1 to p_2, denoted as $l^i(p_1, p_2)$, is the length of the path segment from p_1 to p_2 along the motion direction, which is computed as $l^i(p_1, p_2) = \int_{\theta_1}^{\theta_2} \|dP^i(\theta)/d\theta\|_2 d\theta$.

Definition 2: Given a robot r_i, its speed at time t, denoted as $v^i(t)$, can be described as $v^i(t) = \lim_{\Delta t \to 0} l^i(p(t), p(t + \Delta t))/\Delta t$.

For safety reasons, each robot has a safe radius ρ, and two robots are in a collision if their current positions x and y satisfy $\|x - y\|_2 \leq 2\rho$. Therefore, the safe region of r_i can be described as $\mathbb{A}^i_{2\rho} = \{x | \|x - P^i(\theta)\|_2 \leq 2\rho, \theta \in [0, 1]\}$. Since each robot is fixed to move along a given path, we can guarantee safety only by controlling the motion speed/acceleration. Moreover, deadlocks are widespread in MMRSs, especially in robots with predefined paths [28], [29], [30]. For example, Fig. 1(a) shows four robots crossing an intersection. As given in Fig. 1(b), to avoid collisions, the four robots are in a deadlock and blocked at the intersection forever if they enter the intersection simultaneously without intervention. Hence, the problem studied in this work can be described as follows.

Problem 1: Given an MMRS with predefined paths for robots, determine the real-time motion speeds for robots such that each one can move along its path in a distributed way and guarantee not only collision and deadlock avoidance but also motion smoothness during its motion.

Discrete methods are well-developed in literature to avoid collisions and deadlocks in MMRSs. However, after high-level abstraction, they cannot optimize the continuous motion of robots. It may cause a robot to make sudden changes in speed and even stop and resume its motion frequently (will give

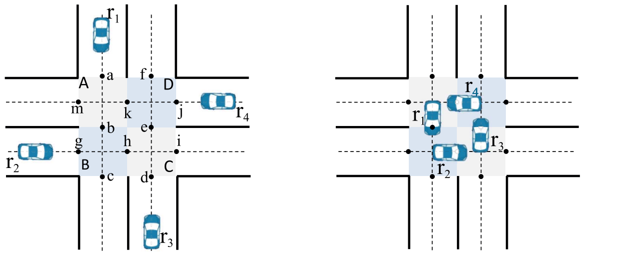

(a) (b)

Fig. 1. Occurrence of deadlocks among four robots. (a) Initial state. (b) Deadlock state.

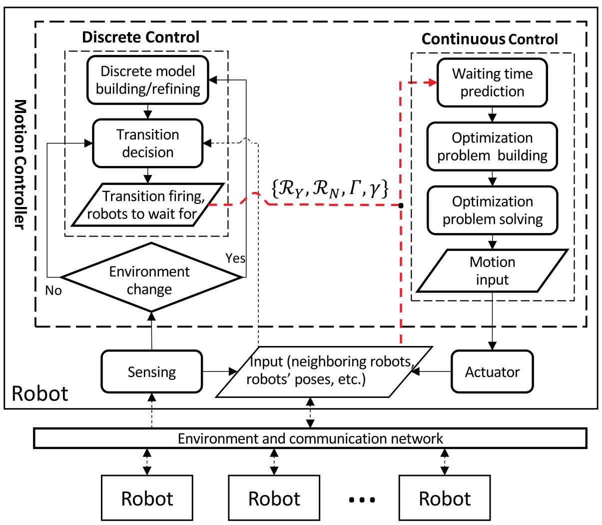

Fig. 2. Framework of the proposed hybrid approach to motion control.

details in our experiments). Such motion is not desired since it is energy-consuming and less comfortable. Hence, this article investigates a hybrid approach to robot motion. Based on state transition systems, a discrete control policy is designed to avoid collisions and deadlocks; based on the MPC strategy, an optimal speed control policy is developed to generate continuous motion.

IV. Design of Hybrid Approach

The architecture of our proposed hybrid motion controller for each robot is shown in Fig. 2. The motion controller first retrieves information about the environment and the states of its neighbors via its onboard sensors and communication network, then computes the control inputs to the actuator. The computation process contains two phases.

1) *Discrete Motion Control:* The robot first builds and refines, if needed, its discrete model based on the path network of the system. Then, by communicating with its neighbors, the robot decides whether the firing of its current transition will cause collisions or deadlocks. The details are given in Section IV-A.
2) *Continuous Speed Optimization:* According to the discrete decision of the first phase, the robot computes its minimal motion time at the current state and optimizes its acceleration for the actuator by building and resolving an optimization problem.

   Section IV-B gives the details. The effectiveness analysis of the proposed approach is given in Section IV-C.

As shown in Fig. 2, the motion accuracy of a robot relies on many aspects, such as the controller, actuator, sensors, and communication network. Since we focus on the design of the motion controller, we assume that other components can always work well. For example, the actuator can respond correctly to its inputs, the sensors can monitor the environment accurately, and the communication network can transmit messages without packet loss and delay. Note, by leveraging the MPC framework, the proposed method can tolerate disturbances in these aspects when the disturbances can be resolved quickly; otherwise, the state-of-the-art technologies [31], [32], [33] can be integrated into the proposed method.

A. Discrete Transition Control

To guarantee the flexibility and efficiency of robot motion, after discretizing a path to discrete states, each time, we only focus on the motion at the current state rather than planning the whole motion along the path. This section describes the building of the discrete transition system model and the discrete transition control. In the following section, we give continuous motion control. We first give a brief review of the path discretization described in [34].

Definition 3 [34]: The collision region between P^i and P^j, denoted as $P^{i,j}$, is a set of segment pairs $(P^i_k, P^j_{k'})$ such that $d(P^i_k, P^j_{k'}) = \inf_{x\in P^i_k} d(x, P^j_{k'}) \leq 2\rho$, where P^i_k and $P^j_{k'}$ are the kth and k'th maximal continuous segments in $P^i \cap \mathbb{A}^j_{2\rho}$ and $P^j \cap \mathbb{A}^i_{2\rho}$, respectively, $k, k' \in \mathbb{N}^+$, and $\mathbb{N}^+$ is the set of positive integers.

Hence, the collision segments of r_i can be described as $\mathcal{P}^i = \cup_j \cup_k \{P^i_k : \exists P^j_{k'},$ such that $(P^i_k, P^j_{k'}) \in P^{i,j}\}$. It is a set of nonoverlapping segments by merging the overlapping ones. The rest of P^i is a set of collision-free segments, called private segments. All collision and private segments form a partition of P^i. An example of the discretization process can be found in the Appendix of the supplementary material and [34].

Each collision segment is abstracted to a discrete collision state. Two collision segments belonging to two different robots are abstracted to the same collision state if the two robots may cause collisions at these two segments, respectively. Each collision-free segment can be further divided into several shorter subsegments based on, e.g., the sensing range. In this way, collision-free segments are abstracted to a set of private states. Note that each robot at a state can retrieve the path segment represented by this state. Let S^i_α and S^i_β be the sets of collision and private states, respectively. Then, $S^i = S^i_\alpha \cup S^i_\beta$. Given a state $s \in S^i$, its represented path segment is denoted as P^i_s, and the tail and head of P^i_s are denoted as A^i_s (called the start of s) and B^i_s (called the end of s), respectively, where robot r_i moves from A^i_s to B^i_s at s. The length of P^i_s, i.e., $l^i(A^i_s, B^i_s)$, is denoted as l^i_s. The set of transitions among the discrete states, denoted as T^i, is determined as follows: Given two states $s_1, s_2 \in S^i$, $(s_1, s_2) \in T^i$ if $B^i_{s_1} = A^i_{s_2}$. Hence, the transition system for r_i is $\mathcal{T}^i = \langle S^i, T^i \rangle$.

According to the discretization process, for any two robots r_i and r_j whose state spaces are S^i and S^j, respectively, there are no collision states such that they are consecutive states in S^i and S^j simultaneously. Hence, our discretization will not cause deadlocks between two robots. However, to guarantee maximal permissive motion, some refined discretization processes may generate such consecutive states (refer to the supplementary file for a detailed example). This may increase control complexity and will be investigated in future work.

Given the transition system $\mathcal{T}^i$, $\forall s \in S^i$, $\mathrm{Pre}_i(s)$ and $\mathrm{Pos}_i(s)$ denote the preceding and succeeding states of s in S^i, respectively, i.e., $(\mathrm{Pre}_i(s), s) \in T^i$ and $(s, \mathrm{Pos}_i(s)) \in T^i$. Let s_c^i be the current state of r_i. Then, $(s_c^i, \mathrm{Pos}_i(s_c^i))$ is the current transition of r_i. At the discrete control phase, r_i determines whether its current transition can be fired without causing collisions or deadlocks. In terms of the discrete model, r_i at s is in a *collision* if there is another robot at s simultaneously, while it is in a *deadlock* if there are a set of robots $r_1, \ldots, r_k$ such that $\mathrm{Pos}_i(s) = s_c^1$, $\mathrm{Pos}_j(s_c^j) = s_c^{j+1}$ for $j = 1, \ldots, k-1$, and $\mathrm{Pos}_k(s_c^k) = s$, where s_c^j is the current state of r_j.

Definition 4: Suppose that r_i is at s. The transition $(s, \mathrm{Pos}_i(s))$ can be enabled if there are no collisions or deadlocks when r_i is at $\mathrm{Pos}_i(s)$. Firing of its current transition $(s, \mathrm{Pos}_i(s))$ transits r_i to $\mathrm{Pos}_i(s)$.

Based on the above definition, a robot is movable if its current transition is enabled, and it cannot transit to its next state until its current transition can be fired. Only when its next state is a collision state may a robot collide with others. Hence, at any time instant, to avoid collisions, each robot needs to retrieve the status of its collision states within its sensing range. For each robot, the status of its collision states can be described by a set of Boolean variables. Let ω^i, $\omega^i = \{\omega^i(s) : s \in S_\alpha^i\}$, be the set of such Boolean variables: $\omega^i(s) = 1$ if s is occupied by other robots; otherwise, $\omega^i(s) = 0$. Thus, the collision avoidance strategy is that: If the Boolean variable related to the next state is 1, then the transition cannot be enabled.

Besides collision avoidance, a robot needs to retrieve the current states of its neighbors via a multihop communication path to avoid deadlocks. Suppose that r_i is at s and $\omega^i(\mathrm{Pos}_i(s)) = 0$. To check whether $(s, \mathrm{Pos}_i(s))$ can be enabled, r_i needs to check further whether its stay at $\mathrm{Pos}_i(s)$ would cause any deadlock. The procedure can be concisely summarized as follows. For more details, please refer to [15]. First, r_i retrieves the status of $\widetilde{s}^i = \mathrm{Pos}_i(\mathrm{Pos}_i(s))$. If another robot, say r_{j_1}, is at $\widetilde{s}^i$, then r_{j_1} is activated to check the status of $\mathrm{Pos}_{j_1}(\widetilde{s}^i)$, denoted as $\widetilde{s}^{j_1}$. Similarly, if $\widetilde{s}^{j_1}$ is also occupied by r_{j_2}, r_{j_2} starts to check the status of $\mathrm{Pos}_{j_2}(\widetilde{s}^{j_1})$. The procedure is terminated when there exists a robot whose next state is $\mathrm{Pos}_i(s)$ or is neither $\mathrm{Pos}_i(s)$ nor occupied. The former means that there exists a deadlock, and $(s, \mathrm{Pos}_i(s))$ cannot be enabled, while the latter means that $(s, \mathrm{Pos}_i(s))$ can be enabled. We denote this deadlock detection process as $\mathcal{D}(r_i, \mathrm{Pos}_i(s))$. $\mathcal{D}(r_i, \mathrm{Pos}_i(s)) = 0$ means that no deadlocks are generated if r_i moves to $\mathrm{Pos}_i(s)$, while $\mathcal{D}(r_i, \mathrm{Pos}_i(s)) = r_j$ means that a deadlock occurs if r_i is at $\mathrm{Pos}_i(s)$, and r_j is the last one in the iteration, i.e., $\mathrm{Pos}_j(s_c^j) = \mathrm{Pos}_i(s)$, where s_c^j is the current state of r_j. In this case, r_i needs to wait for r_j to move away from $\mathrm{Pos}_i(s)$. Note that in this article, to simplify the description, we do not consider higher-order deadlocks described in [16]. However, we can directly replace $\mathcal{D}(r_i, \mathrm{Pos}_i(s))$ by the procedure of higher-order deadlock prediction given in [16].

Since the robots detect collisions and deadlocks in a distributed manner, they may make decisions simultaneously and result in conflicts, i.e., simultaneous firings of enabled transitions result in a collision or deadlock. Hence, an enabled transition sometimes cannot be fired. Indeed, these robots need to negotiate with each other to determine whose transitions can be fired. Before giving the negotiation process, we first introduce the hybrid state of a robot.

Definition 5: The hybrid state of a robot r_i at time t is a quadruple $(s^i(t), p^i(t), v^i(t), l^i(t))$, where $s^i(t) \in S^i$ and $p^i(t) \in P^i_{s^i(t)}$ are the state and position of r_i at time t, respectively, $v^i(t)$ is the speed, and $l^i(t) = l^i(A^i_{s^i(t)}, p^i(t))$ is the path length that r_i has moved at $s^i(t)$.

Suppose that X is a collision region that may exhibit collisions or deadlocks, and $\mathcal{R}_X$ is the set of robots that are moving into/in X at the current instant. All robots in $\mathcal{R}_X$ should negotiate with each other to decide which robots can fire their current transitions. Here, we introduce a heuristic negotiation strategy. The main idea is that the earlier the robot arrives at its next state, the higher priority the robot possesses to make a decision, while the remaining robots make their decisions based on the decisions made by the previous ones. Algorithm 1 shows the negotiation process. First, each robot predicts and broadcasts its time to arrive at its next state (line 2). Then, one by one, each robot in $\mathcal{R}_X$ decides whether it can fire its current transition (lines 3–10) based on the temporary Boolean variables $\nu = \{\nu^i : r_i \in \mathcal{R}_X\}$, where ν^i is initialized to ω^i. Suppose that among the remaining robots in $\mathcal{R}_X$, r_k is the robot with the shortest arriving time to its next state. Based on the Boolean variables ν, r_k checks whether its next state s_x is temporarily occupied or whether there exists a deadlock if it is at s_x. If one of the two conditions is satisfied, r_k cannot fire its current transition. So r_k needs to determine its waiting relation $(r_k, r_j, t_w(k, j))$, including the robot to directly wait for (i.e., r_j) and the possible waiting time (i.e., $t_w(k, j)$) (lines 5–8). Otherwise, r_k can fire its current transition, and the corresponding temporary variable $\nu^k(s_x)$ is changed to 1 (line 10). Finally, r_k is removed from $\mathcal{R}_X$. The negotiation process returns the sets of robots that can and cannot fire their current transitions, i.e., $\mathcal{R}_Y$ and $\mathcal{R}_N$, respectively, and the set of waiting relations, i.e., Γ, of the robots in $\mathcal{R}_N$.

Algorithm 2 shows the decision-making on whether r_i can fire its current transition. It consists of four cases: 1) *Leave to a Private State:* r_i can always fire its current transition to a private state (lines 2 and 3); 2) *Collisions:* the current transition of r_i cannot be enabled when another robot is at the next state (lines 4 and 5); 3) *Deadlocks:* r_i cannot enable its current transition if a deadlock is detected (lines 7 and 8; 4) *Negotiation:* if r_i can move to a collision state, it negotiates with its neighbors based on Algorithm 1 to decide whether the current transition can be fired (lines 10–15). Note that $\gamma = 0$ means that the robot cannot move one step forward due to

Algorithm 1: Negotiation Among the Robots in $\mathcal{R}_X$

Input : Movable robots $\mathcal{R}_X$, and their current hybrid states (s^i, p^i, v^i, l^i) and signals $\{\omega^i\}$.
Output: $\mathcal{R}_Y$: the set of robots that can fire their current transitions; $\mathcal{R}_N$: the set of robots that cannot fire their current transitions; $\Gamma = \{(r_i, r_j, t_w(i,j)) : i \in \mathcal{R}_N\}$: r_i needs to wait for r_j for a time duration $t_w(i,j)$.

Initialization: $\nu = \{\nu^i = \omega^i : \forall i \in \mathcal{R}_X\}$; $\mathcal{R}_Y = \emptyset$; $\mathcal{R}_N = \emptyset$; $\Gamma = \emptyset$;
Compute time to the next state: $t^i = (l^i_{s^i} - l^i)/v^i \quad \forall r_i \in \mathcal{R}_X$;
while $\mathcal{R}_X \neq \emptyset$ **do**
  $r_k = \arg min_{r_i \in \mathcal{R}_X} t^i$; $s_x = Pos_k(s^k)$;
  if $\exists r_j \in \mathcal{R}_X$ *such that* $\nu^j(s_x) = 1 \parallel \mathcal{D}(r_k, s_x) = r_j$ *based on* ν **then**
    $\mathcal{R}_N = \mathcal{R}_N \cup \{r_k\}$;
    $t_w(k,j) = l^j(p^j, B^j_{s_x})/v^j$;
    $\Gamma = \Gamma \cup \{(r_k, r_j, t_w(k,j))\}$;
  else
    $\mathcal{R}_Y = \mathcal{R}_Y \cup \{r_k\}$; $\nu^k(s_x) = 1$;
  $\mathcal{R}_X = \mathcal{R}_X \setminus \{r_k\}$;
return $\{\mathcal{R}_Y, \mathcal{R}_N, \Gamma\}$

Algorithm 2: Decision Making on the Firing of the Current Transition of r_i

Input : Transition system $\mathcal{T}^i$, the current state s, and collision region X containing $Pos_i(s)$.
Output: $\mathcal{R}_Y$: The set of robots that can fire their current transitions; $\mathcal{R}_N$: The set of robots that cannot fire their current transitions; $\Gamma = \{r_k, r_j, t_w(k,j)\}$: The set of waiting relation between two robots and the waiting time; γ: The decision made by r_i.

$\mathcal{R}_Y = \emptyset$, $\mathcal{R}_N = \emptyset$, $\Gamma = \emptyset$;
if $Pos_i(s) \in S^i_\beta$ **then**
  $\gamma = 2$;
else if $\omega^i(Pos_i(s)) = 1$ **then**
  $\gamma = 0$;
else
  if $\mathcal{D}(r_i, Pos_i(s)) \neq 0$ **then**
    $\gamma = 0$;
  else
    $(s, Pos_i(s))$ is enabled and add r_i to $\mathcal{R}_X$;
    $\{\mathcal{R}_Y, \mathcal{R}_N, \Gamma\}$ = Algorithm 1;
    if $r_i \in \mathcal{R}_Y$ **then**
      $\gamma = 2$
    else
      $\gamma = 1$
return $\{\mathcal{R}_Y, \mathcal{R}_N, \Gamma, \gamma\}$.

robot collisions or system deadlocks, $\gamma = 1$ means that the robot is movable but cannot move forward due to the loss of the negotiation process, and $\gamma = 2$ means that the robot can move one step forward.

Once a robot checks that it cannot fire its current transition, i.e., Algorithm 2 outputs $\gamma = 0$ or $\gamma = 1$, the robot needs to optimize its speed such that no collisions or deadlocks are generated when it transits to the next state.

B. Continuous Speed Adjustment

This section describes the MPC-based method to optimize the speed of a robot if it cannot fire its current transition. Once a robot transits to the next state, it has to recompute its speed. It means that the motion derived from the previous state is not feasible anymore. Hence, at any time instant, the prediction horizon is the path from the current position to the end of the path segment at the current state. Since the motion time at each state is varied case by case, we consider the path-horizon MPC process rather than following the conventional time-horizon MPC strategies. Hence, the tuning parameters are the control horizon and the path-length step. In this work, we apply the default one-step control horizon, and the path length of each step is determined such that the robot can fully stop at each step. Even though different tuning methods have been proposed in [35], [36], and [37] to optimize the tuning parameters, it is beyond the scope of this article and will be future work.

At any time t, the state and position of r_i are denoted as $s^i(t)$ and $p^i(t)$, respectively; the path length from the tail $A^i_{s^i(t)}$ to $p^i(t)$ is $l^i(t) = l^i(A^i_{s^i(t)}, p^i(t))$; the speed and acceleration of r_i at t are denoted as $v^i(l^i(t))$ and $a^i(l^i(t))$, respectively. The motion time from $p^i(t)$ to $B^i_{s^i(t)}$ is denoted as $t^i(l^i(t), l^i_{s^i(t)})$. Recall that $l^i_{s^i(t)}$ is the length of P^i at $s^i(t)$. Without ambiguity, we omit the time parameter t in the following description. Given the current time instant t_c, the current hybrid state of r_i can be described as $(s, p^i(l_c), v^i(l_c), l_c)$, where $l_c = l^i(t_c)$. In the sequel, we formulate the optimization problem in the MPC process of r_i at t_c.

First, the kinematic equations can be described as follows:

$$t^i\left(l_c, l^i_s\right) = \int_{l_c}^{l^i_s} \frac{1}{v^i(l)} dl \tag{1}$$

$$\frac{1}{2} v^i\left(l^i_s\right)^2 - \frac{1}{2} v^i(l_c)^2 = \int_{l_c}^{l^i_s} a^i(l) dl. \tag{2}$$

Second, an optimization problem is generated based on the discrete decision and kinematic equations. As described above, a robot r_i may not be able to fire its current transitions due to two situations: 1) the negotiation process forbids the robot to fire its current transition and 2) collisions or deadlocks occur after the firing of the current transition. Once r_i decides that it cannot fire its current transition, it needs to determine the minimal motion time at the current state.

Given the negotiation results, we first compute the minimal motion time under the first situation. From the negotiation process, r_i can retrieve the minimal sequence of waiting robots, which satisfies: 1) the former robots need to wait for the latter

Algorithm 3: Computation of r_i's Waiting Time Based on Its Negotiation Process

Input : $\mathcal{R}_Y$, $\mathcal{R}_N$, and Γ from Algorithm 1.
Output: $t_w(i)$.
1 $\Gamma_i = (r_i, r_j, t_w(i, j))$; $t_w(i) = t_w(i, j)$;
2 **while** $r_j \in \mathcal{R}_N$ **do**
3 Retrieve $\Gamma_j = (r_j, r_k, t_w(j, k))$;
4 $t_w(i) = \max\{t_w(i), t_w(j, k)\}$;
5 $r_j = r_k$;
6 **return** $t_w(i)$.

ones; 2) all robots, except the last one, belong to $\mathcal{R}_N$; and 3) the last robot belongs to $\mathcal{R}_Y$. Based on this sequence, r_i can compute its minimal motion time. The computation procedure is shown in Algorithm 3. According to $(r_i, r_j, t_w(i, j))$, r_i decides that it needs to wait for r_j for a time duration $t_w(i, j)$ (line 1). Hence, r_i can retrieve Γ_j from Γ, based on which r_i further determines the robot, alias r_k, as well as the time duration $t_w(j, k)$, that r_j needs to wait for (line 3). Then, r_i updates its waiting time (line 4) and sets r_j to r_k for the next iteration (line 5). The procedure iterates until r_i finds a robot belonging to $\mathcal{R}_Y$, i.e., a robot that can fire its current transition.

In the sequel, we compute the minimal motion time in the second situation.

Definition 6: Suppose that r_i is required to move to s. We say r_i needs to wait for the move of r_j directly if s is occupied by r_j or $\mathcal{D}(r_i, s) = r_j$. Such a direct waiting relation is denoted as $r_i \preceq r_j$.

Definition 7: A robot r_j is an enable-dependent robot of r_i at state s if $r_i \preceq r_j$ or there exist a sequence of robots $r_{i_1}, \ldots, r_{i_j}$ such that $r_i \preceq r_{i_1} \preceq \ldots \preceq r_{i_j} \preceq r_j$. The set of all enable-dependent robots is denoted as $\mathcal{R}^i(s)$.

r_i can determine the set of enable-dependent robots $\mathcal{R}^i(s)$ in a distributed way via a multihop communication path. First, r_i can determine its direct waiting relation by checking the status of $\mathrm{Pos}_i(s)$ and $\mathcal{D}(r_i, \mathrm{Pos}_i(s))$. If r_i detects that $\mathrm{Pos}_i(s)$ is occupied by another robot r_{i_1} or $\mathcal{D}(r_i, \mathrm{Pos}_i(s)) = r_{i_1}$, i.e., $r_i \preceq r_{i_1}$, r_i sends a message $(r_i, \mathrm{Pos}_i(s))$ to r_{i_1} to inform that r_{i_1} needs to move to $\mathrm{Pos}_{i_1}(\mathrm{Pos}_i(s)) \triangleq \widetilde{s}^{i_1}$. When r_{i_1} receives the message from r_i, r_{i_1} starts to determine its direct waiting relation by checking the status of $\widetilde{s}^{i_1}$ or deriving $\mathcal{D}(r_{i_1}, \widetilde{s}^{i_1})$. Similarly, r_{i_1} can retrieve its direct waiting relation, say $r_{i_1} \preceq r_{i_2}$, and send a notification message to r_{i_2}. So r_{i_2} can begin to retrieve its direct waiting relation. By iterating over all the robots, the process stops when a robot, say r_{i_j}, detects that it can enable all the transitions to the required state. In this way, r_i can retrieve its enable-dependent robots at s, i.e., $\mathcal{R}^i(s) = \{r_{i_1}, \ldots, r_{i_j}\}$. Each robot will also send back its current speed and the path length required to move during the communication, so r_i can predict its minimal motion time at s.

For example, as shown in Fig. 3, r_1 is at s_0 currently. By deriving $\mathcal{D}(r_1, s_1)$, a deadlock would be identified if r_1 moved to s_1, so r_1 retrieves a direct waiting relation $r_1 \preceq r_4$. Hence, r_1 sends a message to r_4, and r_4 needs to retrieve its direct waiting relation with respect to s_5. After checking the status of s_5, r_4 detects that r_5 is at s_5 and sends a message to r_5.

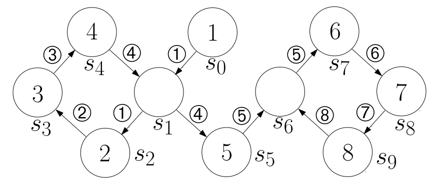

Fig. 3. Illustration of enable-dependent robots. The arrow with ⓝ denotes the transition of r_n.

After receiving the message, r_5 finds that it needs to move to s_6. So r_5 detects whether it is movable to s_6. Since s_6 is not occupied by other robots, r_5 further derives $\mathcal{D}(r_5, s_6)$. Since $\mathcal{D}(r_5, s_6) = r_8$, r_5 sends a message to r_8, and r_8 needs to check whether it can move to the next state of s_6, i.e., checking the status of $\mathrm{Pos}_8(s_6)$. Assume that $\mathrm{Pos}_8(s_6)$ is a private state. Hence, r_8 finally sends back a message, including its speed and path length to move, to r_5. Consequently, r_5 will send back to r_4 this information by adding its speed and path length to move. Similarly, r_4 adds its speed and the path length to move to the message and sends it to r_1. Via such a multihop communication path, r_1 retrieves its enable-dependent robots $\mathcal{R}^1(s_0) = \{r_4, r_5, r_8\}$ and their speeds and path lengths needed to move.

Based on the definition of enable-dependent robots, r_i cannot leave s until all robots in $\mathcal{R}^i(s)$ arrive at the required states. For each robot $r_j \in \mathcal{R}^i(s)$, its current position and speed are p^j and v^j, respectively. During the enable-dependent retrieval process, r_j determines that it needs to move to $\widetilde{s}^j$, which means that r_j is required to move to at least $A^j_{\widetilde{s}^j}$. Hence, the path length that r_j needs to move, denoted as $l^j(i)$, is $l^j(p^j, A^j_{\widetilde{s}^j})$, and the predicted motion time is $t^i_p(j) = l^j(i)/v^j$. In the sequence of enable-dependent robots, the last robot, say r_k, is a movable robot whose minimal motion time $t_w(k)$ can be computed by Algorithm 3. Hence, r_i's minimal motion time at s can be computed as

$$t_w(i) = \max\left\{\max_{r_j \in \mathcal{R}^i(s)} t^i_p(j), t_w(k)\right\}. \tag{3}$$

Hence, the local optimization problem for r_i to compute its optimal speed is shown in (4) in terms of (4a)–(4e). First, the objective function is given in (4a). It consists of two targets: 1) motion smoothness, which means that the robot is expected to move as smoothly as possible to guarantee stability and save energy and 2) motion efficiency, which means that the robot is required to pass through the required states as soon as possible to give way to others. Second, the robot's kinematics and mechanical constraints are given in (4b)–(4d), where $v_{\max}$, $a_{\min}(< 0)$, and $a_{\max}(> 0)$ are the maximal speed, maximal deceleration, and maximal acceleration of the robot, respectively. Finally, the constraint for collision and deadlock avoidance is given in (4e). Indeed, (4e) means that the actual motion time at the current state should be larger than the predicted minimal motion time $t_w(i)$

$$\min_{a^i} \; w_1 \sqrt{\int_{l_c}^{l^i_s} a^i(l)^2 dl} + w_2 \int_{l_c}^{l^i_s} \frac{1}{v^i(l)} dl \tag{4a}$$

subject to: $\forall L \in \left[l_c, l^i_s\right]$

$$\frac{v^i(L)^2}{2} = \frac{v^i(l_c)^2}{2} + \int_{l_c}^{L} a^i(l)dl \tag{4b}$$

$$0 \le v^i(L) \le v_{\max} \tag{4c}$$

$$a_{\min} \le a^i(L) \le a_{\max} \tag{4d}$$

$$t_w(i) \le \int_{l_c}^{l_s^i} \frac{1}{v^i(l)}dl. \tag{4e}$$

Since we focus on path-horizon MPC, the path segment P_s^i can be discretized into a set of equal-length subsegments: $L_0, L_1, \ldots, L_K$, where $L_0 = 0$, $L_K = l_s^i$, $h = l_s^i/K$, and $\forall k \in \mathbb{K} = \{0, 1, \ldots, K\}$, $L_k = kh$. The current discrete instant is denoted as k_c, satisfying $l_c = k_c h$. Based on the path discretization, the control variable $a^i(L)$ is discretized via piece-wise constant: $\forall L \in [L_k, L_{k+1})$, $a^i(L) = a^i(L_k)$. To guarantee safety, the path step length h should satisfy that in any situation, the robot can stop its motion before reaching the next discrete point. Note that in the worst case, the minimal motion distance that the robot needs to stop itself is: $v_{\max}^2/|2a_{\min}|$. Hence, h should satisfy: $h \ge v_{\max}^2/|2a_{\min}|$.

Let $b^i(L) = v^i(L)^2$, $b_k^i = b^i(L_k)$, and $a_k^i = a^i(L_k)$ $\forall k \in \mathbb{K}$. Substituting them into (4b), we have

$$b^i(L) = b_k^i + 2a_k^i(L - L_k) \quad \forall L \in (L_k, L_{k+1}]. \tag{5}$$

Hence

$$\begin{aligned}\int_{l_c}^{l_s^i} \frac{1}{v^i(l)}dl &= \sum_{k=k_c}^{K-1} \int_{L_k}^{L_{k+1}} \frac{1}{v^i(l)}dl \\ &= \sum_{k=k_c}^{K-1} \int_{L_k}^{L_{k+1}} \frac{1}{\sqrt{b_k^i + 2a_k^i(l - L_k)}}dl \\ &= \sum_{k=k_c}^{K-1} \frac{2h}{\sqrt{b_{k+1}^i} + \sqrt{b_k^i}}.\end{aligned}$$

Hence, we can reformulate (4) using a discrete form, namely (6) in terms of

$$\min_{\mathbf{a}^i, \mathbf{b}^i} \; w_1\sqrt{h}\|\mathbf{a}^i\|_2 + w_2 \sum_{k=k_c}^{K-1} \frac{2h}{\sqrt{b_{k+1}^i} + \sqrt{b_k^i}} \tag{6a}$$

$$\text{subject to:} \; \mathbf{A}\mathbf{b}^i - 2h\mathbf{a}^i = 0 \tag{6b}$$

$$b_{k_c}^i = v^i(k_c)^2, \; \mathbf{0} \le \mathbf{b}^i \le v_{\max}^2 \mathbf{1} \tag{6c}$$

$$a_{\min}\mathbf{1} \le \mathbf{a}^i \le a_{\max}\mathbf{1} \tag{6d}$$

$$t_w(i) - \sum_{k=k_c}^{K-1} \frac{2h}{\sqrt{b_{k+1}^i} + \sqrt{b_k^i}} \le 0 \tag{6e}$$

where $\mathbf{b}^i = (b_{k_c}^i, b_{k_c+1}^i, \ldots, b_K^i)^T$ and $\mathbf{a}^i = (a_{k_c}^i, a_{k_c+1}^i, \ldots, a_{K-1}^i)^T$ are control variables, $\mathbf{A} = (A_{kj})_{(K-k_c)\times(K-k_c+1)}$ satisfies $A_{kk} = -1$ and $A_{k,k+1} = 1$ for $k = 1, \ldots, K - k_c$, while others are 0, $v^i(k_c)$ is the speed at the current discrete instant k_c, and $\mathbf{0}$ and $\mathbf{1}$ are the all-zero and all-one vectors with proper dimensions, respectively. Moreover, since there may exist a situation that the robot should stop to wait for others, which means that $\exists k \in \{k_c, k_c + 1, \ldots, K - 1\}$ such that $v_k^i = v_{k+1}^i = 0$, resulting in $1/\sqrt{b_{k+1}^i} + \sqrt{b_k^i}$ is infinite.

Algorithm 4: SCP Procedure to Solve (6)

Input : Current speed $v^i(k_c)$, minimal motion time $t_w(i)$, number of steps K, step length h, maximal number of iterations M, and precision ϵ.

Output: $\mathbf{b}^i$ and $\mathbf{a}^i$.

1 Initialization: $m = 0$, $\mathbf{b}_m^i = \mathbf{0}$, $F_m^i = 0$;
2 **while** $m \le M$ **do**
3   Compute $g(\mathbf{b}_m^i)$ and $\nabla g(\mathbf{b}_m^i)$;
4   Construct approximate convex problem $P(\mathbf{b}_m^i)$;
5   Solve $P(\mathbf{b}_m^i)$;
6   **if** $P(\boldsymbol{b}_m^i)$ *is well solved* **then**
7   Retrieve the optimal solution $\mathbf{b}^i$ and $\mathbf{a}^i$, and the optimal value F^i;
8   **if** $\|\boldsymbol{b}^i - \boldsymbol{b}_m^i\|_2 \le \epsilon$ *or* $|F^i - F_m^i| \le \epsilon$ **then**
9   **return** $\mathbf{b}_i$ and $\mathbf{a}_i$;
10   **else**
11            $m = m + 1$;
12            $F_m^i = F^i$; $\mathbf{b}_m^i = \mathbf{b}^i$;
13   **else**
14        $\forall k \in \{k_c, \ldots, K - 1\}$, $a_k^i = -v^i(k_c)^2/(2 * (K - k_c) * h)$, $b_{k+1}^i = b_k^i - v^i(k_c)^2/(K - k_c)$;
15   **return** $\mathbf{b}^i$ and $\mathbf{a}^i$;

To deal with this situation, we set a large value, e.g., 10^6, to approximately represent $1/0$.

In (4), the objective and constraints satisfy a convex problem except for (6e), which is a difference between two convex functions. Thus, the problem can be solved approximately via sequential convex programming (SCP) [38] or incremental SCP [23]. Since there is only one nonconvex constraint, i.e., (6e), the two methods are with the same efficiency in practice. Hence, the SCP approach is adopted to resolve our problem. In the sequel, we describe the convex approximation of (6) at a given point and give the detailed procedure to solve (6).

Let $g(\mathbf{b}^i) = \sum_{k=k_c}^{K-1} 2h/(\sqrt{b_{k+1}^i} + \sqrt{b_k^i})$, and $\nabla g(\mathbf{b}^i)$ is the gradient of $g(\mathbf{b}^i)$. Its first-order Taylor expansion at a given point $\mathbf{b}_m^i$ can be described as $g(\mathbf{b}_m^i) + \nabla g(\mathbf{b}_m^i)^T(\mathbf{b}^i - \mathbf{b}_m^i)$. Hence, the approximate convex problem at $\mathbf{b}_m^i$, denoted as $P(\mathbf{b}_m^i)$, can be described as follows:

$$\min_{\mathbf{a}^i, \mathbf{b}^i} \; w_1\sqrt{h}\|\mathbf{a}^i\|_2 + w_2 \sum_{k=k_c}^{K-1} \frac{2h}{\sqrt{b_{k+1}^i} + \sqrt{b_k^i}}$$

$$\begin{aligned}\text{subject to:} \; & \mathbf{A}\mathbf{b}^i - 2h\,\mathbf{a}^i = 0, b_{k_c}^i = v^i(k_c)^2, P(\mathbf{b}_m^i) \\ & \mathbf{0} \le \mathbf{b}^i \le v_{\max}^2\mathbf{1}, \; a_{\min}\mathbf{1} \le \mathbf{a}^i \le a_{\max}\mathbf{1} \\ & t_w(i) - \left[g\left(\mathbf{b}_m^i\right) + \nabla g\left(\mathbf{b}_m^i\right)^T\left(\mathbf{b}^i - \mathbf{b}_m^i\right)\right] \le 0.\end{aligned}$$

Hence, (6) can be resolved iteratively by resolving $P(\mathbf{b}_m^i)$. Algorithm 4 gives the detailed SCP procedure. lines 3–12 are the iteration process of SCP, while lines 13–15 focus on the situation that $P(\mathbf{b}_m^i)$ cannot find an optimal solution at an iteration. For each iteration, the value of $\mathbf{b}_m^i$ is set as the optimal solution of the former iteration (line 12). We give two stopping criteria of the iteration process: 1) the number of iterations reaches the maximal one (line 2), and 2) the difference between two successive solutions is less than the given precision (line 8). The iteration is stopped if either of them is satisfied. If $P(\mathbf{b}_m^i)$ cannot find an optimal solution at an iteration, we generate a feasible solution to stop the robot before it reaches the end of the current state (lines 13–15).

Finally, Algorithm 5 shows the complete hybrid MPC-based motion control at an arbitrary state based on Algorithms 2–4. line 3 performs the discrete decision-making to determine whether the robot can enable or fire its current transition. lines 4–6 compute the minimal motion time if the robot cannot enable its current transition due to collision and deadlock avoidance, while lines 7 and 8 compute the minimal motion time if the robot can enable its current transition but does not win the right to fire the transition during negotiation. Once the minimal motion time is obtained, the robot computes the optimal motion at the current step (line 11). Note that the computation returns a sequence of motion commands in the future, but the robot applies only the first one to move to the next discrete point (lines 12–14). Once it arrives at the next point, the robot updates its status (lines 15 and 16) and starts a new iteration.

It is worth noting that the computational complexity of Algorithms 2 and 3 is $O(n)$, while Algorithm 4 includes the computation of a finite number of convex optimization problems, each of which can be resolved approximately in polynomial time with respect to the number of variables and the size of the optimization problem [23], [39]. Hence, at each instant, Algorithm 5 can be resolved with a polynomial-time complexity with respect to the numbers of robots and prediction steps. Moreover, according to the scalability metric defined in [40], the system is scalable under Algorithm 5. In our situation, given a system with N robots, the value rate produced by the system is defined as the rate of motion task finished per time unit, computed as $\mathbb{V}(N) = Ne_0$, where e_0 is the motion efficiency of each robot, and the cost rate of the system is defined as the maximal communication time of a robot to receive the responses from its neighbors to each request, computed as $\mathbb{C}(N) = (N-1)T_{\text{com}}$, where T_{com} is the maximal communication time between any pair of robots. As there are at least two robots in an MMRS, the scalability metric $\varphi(N)$ can be described as $\varphi(2, N)$. Hence, we have

$$\begin{aligned}\varphi(N) = \varphi(2, N) &= \frac{\mathbb{V}(N)/\mathbb{C}(N)}{\mathbb{V}(2)/\mathbb{C}(2)} \\ &= \frac{Ne_0/((N-1)T_{\text{com}})}{2e_0/T_{\text{com}}} = \frac{1}{2} + \frac{1}{2(N-1)}\end{aligned} \tag{7}$$

and $\lim_{N\to\infty}\varphi(N) = 1/2$. Therefore, the system is scalable.

C. Effectiveness Analysis of the Hybrid Method

This section analyzes the effectiveness of the proposed hybrid method. Given a robot r_i, let $t_p(i)$ and $\bar{t}^i$ be the predicted and actual motion time that r_i needs to move at the current state. Moreover, let $F_1^i = w_1\sqrt{h}\|\mathbf{a}^i\|_2$ and $F_2^i = w_2\sum_{k=k_c}^{K-1} 2h/(\sqrt{b_{k+1}^i}+\sqrt{b_k^i})$, then objective function (6a) can be written as $F^i = F_1^i + F_2^i$.

Lemma 1: If r_i can fire its current transition, then $t_p(i) \geq \bar{t}^i$.

Proof: If r_i can fire its current transition, (6e) does not need to be considered. In this situation, decelerated motion is not

---

Algorithm 5: MPC-Based Control for r_i's Motion at s

Input : Mechanical constraints: $v_{\max}$, $a_{\max}$, and $a_{\min}$, hybrid state at the tail of P_s^i: $(s, p_0^i, v_0^i, 0)$, and the precision: ϵ.

1 Initialization: Path discretization by setting h and K, $k_c = 0$;
2 **while** $k_c < K$ **do**
3 $\{\mathcal{R}_Y, \mathcal{R}_N, \Gamma, \gamma\}$ = Algorithm 2;
4 **if** $\gamma = 0$ **then**
5 Determine enable-dependent robots $\mathcal{R}^i(s)$;
6 Compute the minimal motion time $t_w(i)$ via (3);
7 **else if** $\gamma = 1$ **then**
8 $t_w(i)$ = Algorithm 3;
9 **else if** $\gamma = 2$ **then**
10 $t_w(i) = 0$;
11 Call Algorithm 4 and return $\mathbf{b}^i, \mathbf{a}^i$;
12 $a_{k_c}^i = \mathbf{a}^i(1)$; /* select the first value. */
13 $t[k_c \to k_c + 1] = ([\sqrt{\mathbf{b}^i(2)} - \sqrt{\mathbf{b}^i(1)}]/a^i[k_c])$;
14 Move to L_{k_c+1} with acceleration $a_{k_c}^i$ and speed $v_{k_c}^i$;
15 $k_c = k_c + 1$ and $v_{k_c}^i = \sqrt{\mathbf{b}^i(2)}$;
16 Update the hybrid state $(s, p_{k_c}^i, v_{k_c}^i, L - k_c h)$.

---

an optimal solution. Indeed, let F^i and $\widehat{F}^i$ be the objective values under constant and decelerated motion with respect to the current speed, respectively. First, it is clear that $F_1^i = 0$, while $\widehat{F}_1^i > 0$. Second, the motion time to the same position under a decelerated motion is larger than that under a constant motion, which means $F_2^i < \widehat{F}_2^i$. Thus, $F^i < \widehat{F}^i$. It means that in this situation, r_i should move with its current speed or an accelerated speed. Hence, $t_p(i) \geq \bar{t}^i$. ■

Based on Lemma 1, we can derive the following lemma.

Lemma 2: If a robot can move at its current speed v_c, its optimal motion is either a constant or an accelerated motion with respect to v_c.

Lemma 3: The motion under the solution of problem (6) can guarantee the avoidance of robot collisions and system deadlocks.

Proof: Suppose that r_{i_0} cannot transit to the next state at its current state s, and the sequence of its enable-dependent robots is $\mathcal{R}^i(s) = \{r_{i_1}, r_{i_2}, \ldots, r_{i_j}\}$, where r_{i_k} needs to wait for the move of $r_{i_{k+1}}$ for $k = 1, 2, \ldots, j-1$, and r_{i_j} can fire its current transition. r_{i_k}'s real motion time to the required position is denoted as $\bar{t}^{i_k}$. Based on Lemma 1, we have $t_p(i_j) \geq \bar{t}^{i_j}$. If $t_p(i_{j-1}) \geq t_p(i_j)$, $r_{i_{j-1}}$ can move at least with its current speed based on Lemma 2. Moreover, based on (6e), $\bar{t}^{i_{j-1}} \geq t_p(i_j)$. Thus, we have $t_p(i_{j-1}) \geq \bar{t}^{i_{j-1}} \geq t_p(i_j) \geq \bar{t}^{i_j}$; If $t_p(i_{j-1}) < t_p(i_j)$, $r_{i_{j-1}}$ needs to decelerate its motion based on its own optimal problem (6). In this case, $r_{i_{j-1}}$'s optimal solution should reach the boundary of its own constraint (6e), implying $\bar{t}^{i_{j-1}} = t_p(i_j) > t^{i_j}$. Hence, the real motion time of $r_{i_{j-1}}$ satisfies $\max\{t_p(i_{j-1}), t_p(i_j)\} \geq \bar{t}^{i_{j-1}} \geq \bar{t}^{i_j}$.

Suppose that $r_{i_{k+1}}$ satisfies $\max\{t_p(i_{k+1}), \ldots, t_p(i_j)\} \geq \bar{t}^{i_{k+1}} \geq \ldots \geq \bar{t}^{i_j}$. Let us consider r_{i_k}. If $t_p(i_k) \geq \max\{t_p(i_{k+1}), \ldots, t_p(i_j)\}$, r_{i_k} at least can move at its current speed based on its own (6). Thus, we have $t_p(i_k) \geq \bar{t}^{i_k} \geq \max\{t_p(i_{k+1}), \ldots, t_p(i_j)\} \geq \bar{t}^{i_{k+1}}$. Note that in this case $t_p(i_k) = \max\{t_p(i_k), t_p(i_{k+1}), \ldots, t_p(i_j)\}$. If $t_p(i_k) < \max\{t_p(i_{k+1}), \ldots, t_p(i_j)\}$, r_{i_k} needs to decelerate its motion.

In this case, r_{i_k}'s optimal solution should reach the boundary of its own constraint (6e). This means $\bar{t}^{i_{j-1}} = \max\{t_p(i_{k+1}), \ldots, t_p(i_j)\} > \bar{t}^{i_{k+1}}$. In conclusion, we have $\max\{t_p(i_k), \ldots, t_p(i_j)\} \geq \bar{t}^{i_k} \geq \cdots \geq \bar{t}^{i_{k+1}} \geq \cdots \geq \bar{t}^{i_j}$.

Based on the method of induction, we have that $\bar{t}^{i_0} \geq \bar{t}^{i_k} \geq \cdots \geq \bar{t}^{i_{k+1}} \geq \cdots \geq \bar{t}^{i_j}$. It means that when r_{i_0} arrives at the end of its current state, its enable-dependent robots have left their required positions. Hence, r_{i_0} can transit to its next state without any collision or deadlock. ■

Lemma 4: Algorithm 4 can always return a suboptimal, if not optimal, solution to (6).

Proof: Based on our discretization, each robot can stop its motion from L_{k_c} to L_K. Thus, when $P(\mathbf{b}_m^i)$ fails to find an optimal solution, lines 13–15 in Algorithm 4 can guarantee a feasible solution of (6). Otherwise, the optimal solution of $P(\mathbf{b}_m^i)$ at $\mathbf{b}_m^i$ is a suboptimal, if not optimal, solution of (6). Indeed, for a convex function $f(\mathbf{x})$, given an arbitrary point $\mathbf{x}_0$, we have $\forall \mathbf{x}, f(\mathbf{x}) \geq f(\mathbf{x}_0) + \nabla f(\mathbf{x}_0)^T(\mathbf{x} - \mathbf{x}_0)$. Since $g(\mathbf{b}^i) = \sum_{k=k_c}^{K-1} 2h/(\sqrt{b_{k+1}^i} + \sqrt{b_k^i})$ is a convex function, we have $g(\mathbf{b}^i) \geq g(\mathbf{b}_m^i) + \nabla g(\mathbf{b}_m^i)^T(\mathbf{b}^i - \mathbf{b}_m^i)$. Hence, $t_w(i) - g(\mathbf{b}^i) \leq t_w(i) - [g(\mathbf{b}_m^i) + \nabla g(\mathbf{b}_m^i)^T(\mathbf{b}^i - \mathbf{b}_m^i)]$. Compared with $P(\mathbf{b}_m^i)$ and (7), the optimal solution of (7) is a feasible solution of $P(\mathbf{b}_m^i)$. The suboptimality can be derived directly from the local convergence of SCP [41]. ■

Theorem 1: Under Algorithm 5, each robot can move under a suboptimal, if not optimal, motion without causing collisions and deadlocks.

Proof: It is easily proved based on Lemmas 3 and 4 since Lemma 3 guarantees collision and deadlock avoidance at each time instant of the MPC procedure and Lemma 4 guarantees a suboptimal, if not optimal, motion. ■

V. Simulation Study

In the sequel, we show some simulation results and a real-world experiment for MMRSs under the control of the proposed hybrid method. Our simulations are implemented by MATLAB with the CVX toolbox and the MOSEK solver on the HP Z440 workstation, whose CPU and memory are Intel Xeon E5-1650 v3 @ 3.50 GHz and 16.0 GB, respectively. Our real-world experiment is done with three TurtleBot3 Waffle Pi robots.

A. Simulation Results With Our Hybrid Control Method

Our first system for simulation is given in Fig. 1(a), whose transition system is shown in Fig. 4(a). The private states s_5, s_6, s_7, and s_8 represent the path segments from the vehicles' current locations to the intersection boundaries a, g, d, and j, respectively, and they have the same path length 3ρ, where $\rho = 100$ distance units. r_1's collision path segments ab and bc are modeled as the collision states s_1 and s_2, respectively. r_2's collision path segments gh and hi are represented by the collision states s_2 and s_3, respectively. Similarly, de and ef are modeled as s_3 and s_4 for r_3, and jk and km are modeled as s_4 and s_1 for r_4. We assume that all collision path segments have the same path length 4ρ. Moreover, the mechanical constraints of the four

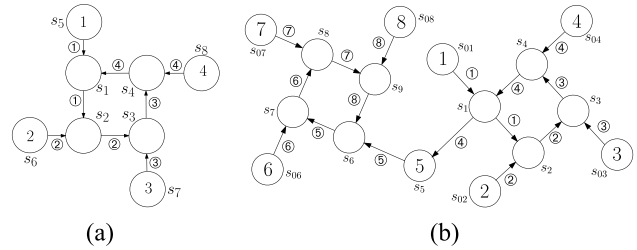

Fig. 4. Transition systems studied in the experiments. (a) Transition system. (b) More sophisticated transition system.

vehicles are $v_{\max} = 100$ distance units/sec, $a_{\min} = -150$ distance units/sec^2, and $a_{\max} = 150$ distance units/sec^2. The discretization step is $h = 100/3$ distance units, generating 9 and 12 discrete steps at a private state and a collision state, respectively. During our simulation, the computation time of each iteration in Algorithm 4 is about 0.44 s, and most of the computation can be convergent in two iterations. However, the number of iterations generated at some instances is larger than 10. Note that the number of iterations highly depends on the initial solution. It will be our future work to improve the quality of the initial solution.

In the simulation, the initial states of r_1, r_2, r_3, and r_4 are s_5, s_6, s_7, and s_8, respectively, and their initial speeds are 60, 50, 40, and 30 distance units/sec, respectively. Fig. 5 shows the speed profile of the four robots during their motion, whether each gray dot denotes that there is a state transition at the corresponding time instant. First, since s_1, s_2, s_3, and s_4 form a collision region X, the four vehicles need negotiation according to Algorithm 1. Based on the negotiation process, since r_1, r_2, and r_3 have higher speed than r_4, they can fire their current transitions and move into X first, while r_4 should wait for the move of r_3. Hence, as shown in Fig. 5, at the start, r_1, r_2, and r_3 continue their motion at their current speeds, while r_4 slows down.

During the system's evolution, r_1 first transits to s_1 at time t_1. Since r_2 will arrive at s_2 earlier than r_1, the negotiation among r_1–r_4 decides that r_1 should wait for r_2's move from s_2. Note that r_4 is still waiting for r_3. Hence, r_1 slows down its motion at t_1, as shown in Fig. 5. Subsequently, r_2 transits to s_2 at t_2. Since r_3 will transit to s_3 earlier than r_2, r_2 needs to wait for r_3 at s_2. Hence, r_2 also starts to decrease its speed at t_2. At time instant t_3, r_1, r_2, and r_3 arrive at the end of s_1, s_2, and s_3 simultaneously. Thus, when r_3 transits to s_4, r_2 transits to s_3 and r_1 to s_2. Based on their optimal objectives, r_1 first accelerates and then keeps a constant speed, while r_2 moves with its current speed. Note that r_4 still decelerates to avoid collision with r_3. At time instant t_4, r_3 arrives at the end of s_4 and then moves away. So r_4 transits to s_4. Since it does not need to wait for any robot anymore, r_4 first speeds up and then keeps a uniform motion. During the whole simulation, the minimal distance between any two robots is around five distance units (between r_3 and r_4). The simulation video can be found at https://yuanzhou-yzhou.github.io/hybrid-motion/.

In conclusion, from the speed profiles given in Fig. 5, we can find that during the motion in the intersection, each robot can avoid collisions and deadlocks by adjusting its speed while keeping its motion as smooth as possible.

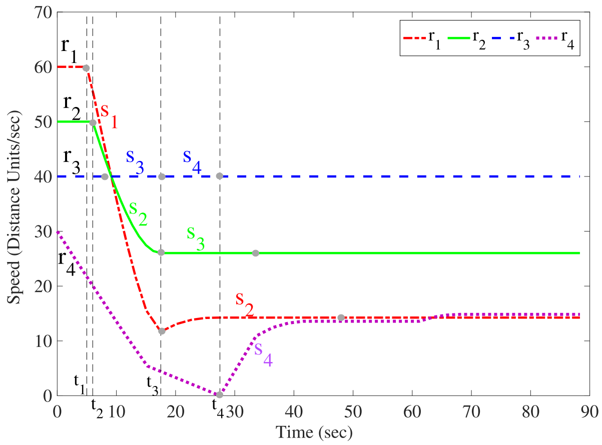

Fig. 5. Speed of the four robots in the simulation.

B. Comparison With Discrete Control

To illustrate the efficiency of our method, we compare the robot motion computed by our method and the discrete one. For the discrete method, we introduce a straightforward way to control robot motion at a discrete state: The robot first moves at a constant speed; when the robot checks that it cannot move to the next state, it slows down its motion at the largest deceleration and stops at the end of the state. Moreover, the robots transit to a state on a first-arrive first-transit basis as long as its transition does not cause collisions or deadlocks. In this way, we can simulate the motion of the robots in Fig. 4(a). The results are given in Fig. 6, where (a) and (b) show the state transitions and speed profiles, respectively.

From Fig. 6(a), we can find that r_1, r_2, and r_3 sequentially move into the intersection and arrive at s_1, s_2, and s_3, respectively, while r_4 is still at s_8. When r_4 reaches the end of s_8, its discrete controller checks a deadlock and thus stops the robot's motion immediately at the largest deceleration. Hence, as given in Fig. 6(b), r_4 stops its motion at the end of s_8 at time t_1, while r_1, r_2, and r_3 are still moving at s_1, s_2, and s_3, respectively. Near the end of s_1, r_1's discrete controller predicts that r_2 is still at s_2 when r_1 reaches the end of s_1. Thus, r_1 slows down its motion and stops at the end of s_1 at time t_2, as given in Fig. 6(b). Similarly, r_2's controller predicts that when r_2 arrives at the end of s_2, r_3 is still at s_3, so r_2 slows down its motion with its maximal deceleration and completely stops at time t_3. r_3 continues its motion at s_3 until t_4, at which the robot transits to s_4. After r_3 moves to s_4, r_2 can move to s_3, and then r_1 can move to s_2, but r_4 is still stopping at s_8. Hence, r_1 and r_2 resume their motion to their former speeds with the maximal acceleration and then move at constant speeds. At time t_5, r_3 moves away from s_4, so r_4 can move forward. Speeding up with its maximal acceleration, r_4 resumes its motion and then moves at a constant speed.

From Figs. 5 and 6(b), we can find that the motion generated by the proposed hybrid method has much fewer stops and jerks than that generated by discrete control. Hence, the proposed method can generate smooth motion for robots. When a robot detects that a collision or deadlock occurs if it were at the next state, the robot should wait for a proper duration at its current state such that other robots can give way to it. In discrete control, the robot adjusts its speed only when

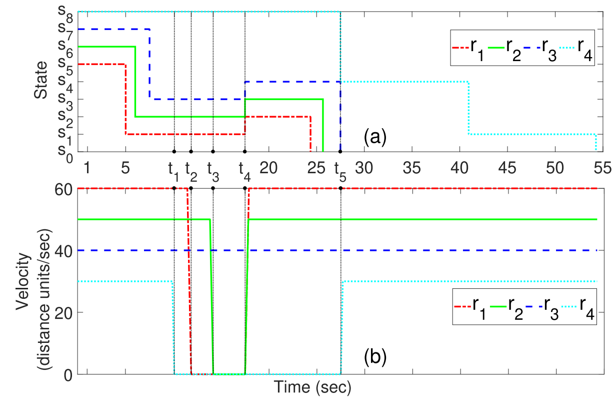

Fig. 6. Simulation results under only discrete control.

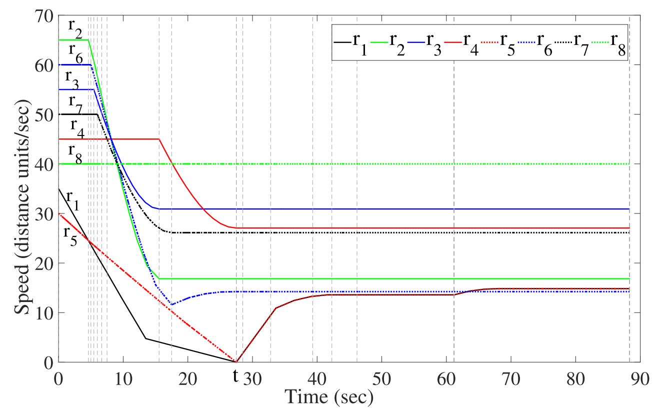

Fig. 7. Speed evolution of the robots.

it is near the end of the state. It means the robot has a shorter time and path length to adjust its speed, so it has to slow down at its maximal deceleration and stop at the end of the current state. In our method, the robot first predicts whether it can transit to the next state at any discrete point and then optimizes its speed based on the predicted minimal motion time. In this way, the robot can smoothly arrive at the end of the state with an intelligently tuned smooth speed change. Hence, our approach leads to the advantages of fewer stops and jerks.

C. More Complex Scenario

This section studies a more complex system to show the efficiency of the proposed hybrid method. As given in Fig. 4(b), there are eight robots, r_1–r_8, in the system, and they are currently at their private states s_{01}–s_{08}. The system parameters in this scenario are the same as the system described in Section V-A. The initial speeds of r_1–r_8 are 35, 65, 55, 45, 30, 60, 50, and 40 distance units/sec, respectively. Clearly, the collision region in this scenario is $X = \{s_1, s_2, \ldots, s_9\}$.

Fig. 7 shows the speed profiles of these robots. The vertical lines indicate the time instances when the robots fire their transitions. First, based on the negotiation process, r_1 and r_6 need to wait for r_4 and r_8, respectively. Hence, the hybrid controllers decide that r_1 and r_6 should slow down, as shown in Fig. 7. Second, r_2 first transits to s_2 at the time denoted by the first vertical line. When it arrives at s_2, r_2 should slow down since the negotiation process finds that r_3 moves to s_3 earlier.

TABLE I
COMPARISONS OF THE MOST RELEVANT METHODS

Metric	Method		
	M_1 ([13])	M_2 ([14])	M_I (Ours)
Addressed Deadlock	Decision Deadlocks	Decision Deadlocks	Physical Deadlocks
Deadlock Resolution	Compute motion priorities based on different motion time	Apply the predefined priorities	Adjust each robot's speed individually
Motion Manner	Distributed Computation, Synchronous Motion	Distributed Computation, Synchronous Motion	Distributed Computation, Asynchronous Motion
Computation Cost	$\mathcal{C}(M_1) \leq \mathcal{C}(M_2) \leq \mathcal{C}(M_I)$		
Permissive Motion	$\mathcal{S}(M_I) \geq \mathcal{S}(M_2) \geq \mathcal{S}(M_1)$		

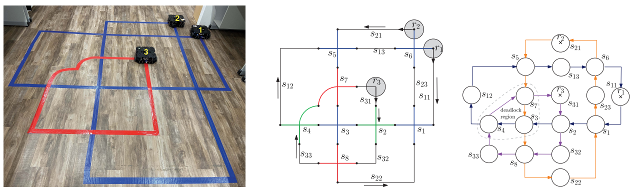

(a) (b) (c)

Fig. 8. Physical experimental scenario. (a) Real-world scenario. (b) Path diagram. (c) LTS.

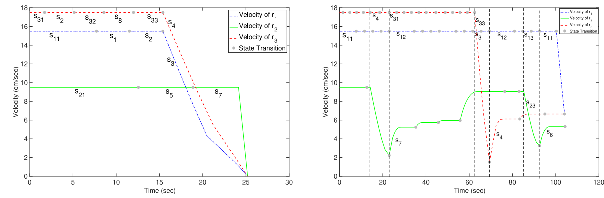

(a) (b)

Fig. 9. Speed profiles of the robots under different controllers. (a) Collision avoidance controller. (b) Hybrid controller.

Next, r_6 transits to s_7 and then reduces its speed since r_7 will reach s_8 earlier. Sequentially, r_3, r_7, and r_4 transit to their next states and decrease their speeds to avoid collisions. Similarly, we can analyze the motion of these robots at different time instants. When r_8 arrives at its private state at time t, r_5 can move to s_6, and r_4 to s_5, resulting in r_1's transiting to s_1. Hence, the states of these robots at time t are s_1, s_3, s_4, s_5, s_6, s_8, s_9, and the private state pvt, respectively. From t, all robots can move forward directly, so r_1 and r_5 need to resume their motion. Since their parameters are the same, their optimal speeds are the same. It can be seen in Fig. 7.

D. Real-World Implementation

In this section, we evaluate our algorithm with three physical TurtleBot3 Waffle Pi robots. Each robot is equipped with a Raspberry Pi computer with Ubuntu 16.04 and ROS Kinetic, a Raspberry Pi Camera Module 2, and a 360 Laser Distance Sensor LDS-01. Each robot is equipped with a remote computer to execute the control algorithms and generate motion commands. The physical paths of the three robots are shown in Fig. 8. The initial speeds of the three robots are 5.5 cm/sec, 9.5 cm/sec, and 17.5 cm/sec, respectively. We first conduct an experiment where each robot is controlled with only the collision avoidance algorithm and then conduct the second experiment where each robot is controlled by our proposed controller. Fig. 9 gives the speed profiles of the three robots under the two experiments. The results show that the three robots are in a deadlock in the first experiment, while they can move persistently in the second experiment. The detailed experimental results can be found at https://yuanzhou-yzhou.github.io/hybrid-motion/.

VI. DISCUSSION AND COMPARISON

In this section, we compare our method (denoted as M_I) with the two most relevant methods: [13] and [14], denoted as M_1 and M_2, respectively. We compare these methods from the perspectives of deadlock to be addressed, resolution methods, computation cost, and permissive motions. The comparison results are shown in Table I, where $\mathcal{C}()$ and $\mathcal{S}()$ denote the computation cost and permissive motions, respectively. The main difference between their works and ours is that they focus on decision deadlocks, while we aim to deal with physical deadlocks, which are more serious and difficult to resolve.

Indeed, there is a tradeoff between the computation cost and permissive motion. M_1 abstracts intersecting path segments into a set of nonadjacent collision zones. It means that there is at least one collision-free position for any robot between any two collision zones. Hence, no physical deadlocks will occur during collision avoidance. This method is efficient but may forbid many permissive motions. M_2 studies conflict resolution in road junctions. Instead of partitioning the paths directly, it divides an intersection into a set of collision zones and then computes the time duration to pass the collision zones for each vehicle along its path. Based on the time duration, M_2 can determine the temporal advantages of the vehicles, which determine the orders of vehicles to pass through collision zones. Similar to M_1, there may exist cycles in the temporal advantages, resulting in decision deadlocks. They can be resolved by the predefined vehicle priorities. It is worth noting that decision deadlocks may not result in physical deadlocks (an example will be given later). Hence, some feasible motions are also forbidden. In our method, we study physical deadlock avoidance directly. It means that only when its motion to the next state causes a physical deadlock does a robot need to change its speed profile.

We show an example to demonstrate the difference in permissive motions of the three methods. As shown in Fig. 10, there are three robots passing through an intersection divided into five collision zones: s_1–s_5. Based on the method in [13], the zones are abstracted as a single collision zone. At any time instant, only one robot can be at one of these zones. Suppose that the current time durations of robots at their states are $T_0^1 = [0, 2]$, $T_1^1 = [2, 4]$, $T_2^1 = [4, 6]$, $T_3^1 = [6, 8]$, $T_4^1 = [8, 10]$; $T_4^2 = [0, 3]$, $T_5^2 = [3, 6]$, $T_2^2 = [6, 9]$; $T_5^3 = [0, 2]$, $T_3^3 = [2, 5]$, $T_1^3 = [5, 8]$, where T_j^i means the time

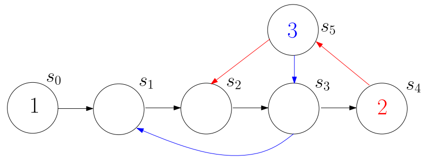

Fig. 10. Example for the comparison of different methods, where $r_1 : s_0 \to s_1 \to s_2 \to s_3 \to s_4$, $r_2 : s_4 \to s_5 \to s_2$, and $r_3 : s_5 \to s_3 \to s_1$.

duration for r_i to pass through s_j. Based on the method in [14], the original temporal advantages are $r_1 \to r_2 \to r_3 \to r_1$. After deadlock resolution, the sequence of yieldings is r_1 yields r_2 and r_3, and r_2 yields r_3. Hence, r_1 cannot move to s_1 until r_3 leaves s_1. However, in our method, the original temporal advantages are allowable since there are no physical deadlocks. Based on our method, after 2 time units, r_1 enters s_1, and r_3 enters s_3, while after 3 time units, r_2 moves to s_5. Before r_3 enters s_1, r_1 has left s_1 and entered s_2. When r_1 leaves s_2 after 6 time units, r_2 is ready to move to s_2. Hence, all the robots can move at their current speed profiles.

VII. Conclusion

This article investigates motion control of MMRSs where each robot is required to move along a fixed path and proposes a distributed, real-time, and hybrid method. First, the motion of each robot is modeled as a discrete transition system, and an online distributed policy is designed to determine whether a robot can fire its current transition. Third, an MPC-based policy is proposed to optimize the speed of each robot at each discrete state to obey the discrete decision. Each optimization problem constructed at this phase only contains the mechanical constraints of the robot and the time-related constraint generated from the discrete control phase. In this way, we can reduce the scale of the local optimization problem significantly at any step.

In the future, we will investigate the implementation of our method on real robots. Our approach will be extended to systems where a robot has multiple paths or systems operating in a free environment with complex tasks (e.g., high-dynamics formation [42]) or mechanisms (e.g., soft robots [43]). Another interesting topic is to investigate systems where a path has multiple robots. Moreover, optimization can be conducted in the negotiation process of the discrete control part.

References

[1] C. Kitts and M. Egerstedt, "Design, control, and applications of real-world multirobot systems [from the guest editors]," *IEEE Robot. Autom. Mag.*, vol. 15, no. 1, p. 8, Mar. 2008.

[2] A. Khamis, A. Hussein, and A. Elmogy, "Multi-robot task allocation: A review of the state-of-the-art," in *Cooperative Robots and Sensor Networks*, A. Koubâa and J. R. Martínez-de Dios, Eds. Berlin, Germany: Springer, 2015, pp. 31–51.

[3] S. L. Smith, M. Schwager, and D. Rus, "Persistent robotic tasks: Monitoring and sweeping in changing environments," *IEEE Trans. Robot.*, vol. 28, no. 2, pp. 410–426, Apr. 2012.

[4] M. Kloetzer and C. Belta, "Temporal logic planning and control of robotic swarms by hierarchical abstractions," *IEEE Trans. Robot.*, vol. 23, no. 2, pp. 320–330, Apr. 2007.

[5] M. Kloetzer, C. Mahulea, and R. Gonzalez, "Optimizing cell decomposition path planning for mobile robots using different metrics," in *Proc. Int. Conf. Syst. Theory, Control Comput.*, Cheile Gradistei, Romania, Oct. 2015, pp. 565–570.

[6] M. Pivtoraiko and A. Kelly, "Kinodynamic motion planning with state lattice motion primitives," in *Proc. IEEE/RSJ Int. Conf. Intell. Robots. Syst.*, San Francisco, CA, USA, Sep. 2011, pp. 2172–2179.

[7] P. Bhattacharya and M. L. Gavrilova, "Roadmap-based path planning—Using the Voronoi diagram for a clearance-based shortest path," *IEEE Robot. Autom. Mag.*, vol. 15, no. 2, pp. 58–66, Jun. 2008.

[8] T. Lai, F. Ramos, and G. Francis, "Balancing global exploration and local-connectivity exploitation with rapidly-exploring random disjointed-trees," in *Proc. IEEE Int. Conf. Robot. Autom.*, Montreal, QC, Canada, May 2019, pp. 5537–5543.

[9] L. Huang, M. Zhou, K. Hao, and H. Han, "Multirobot cooperative patrolling strategy for moving objects," *IEEE Trans. Syst., Man, Cybern., Syst.*, vol. 53, no. 5, pp. 2995–3007, May 2023.

[10] L. Huang, M. Zhou, and K. Hao, "Non-dominated immune-endocrine short feedback algorithm for multi-robot maritime patrolling," *IEEE Trans. Intell. Transp. Syst.*, vol. 21, no. 1, pp. 362–373, Jan. 2020.

[11] L. Huang, M. Zhou, K. Hao, and E. Hou, "A survey of multi-robot regular and adversarial patrolling," *IEEE/CAA J. Automatica Sinica*, vol. 6, no. 4, pp. 894–903, Jul. 2019.

[12] Y. Zhou, H. Hu, Y. Liu, S.-W. Lin, and Z. Ding, "A real-time and fully distributed approach to motion planning for multirobot systems," *IEEE Trans. Syst., Man, Cybern., Syst.*, vol. 49, no. 12, pp. 2636–2650, Dec. 2019.

[13] D. E. Soltero, S. L. Smith, and D. Rus, "Collision avoidance for persistent monitoring in multi-robot systems with intersecting trajectories," in *Proc. IEEE/RSJ Int. Conf. Intell. Robots. Syst.*, San Francisco, CA, USA, Sep. 2011, pp. 3645–3652.

[14] C. Liu, C.-W. Lin, S. Shiraishi, and M. Tomizuka, "Distributed conflict resolution for connected autonomous vehicles," *IEEE Trans. Intell. Veh.*, vol. 3, no. 1, pp. 18–29, Mar. 2018.

[15] Y. Zhou, H. Hu, Y. Liu, and Z. Ding, "Collision and deadlock avoidance in multirobot systems: A distributed approach," *IEEE Trans. Syst., Man, Cybern., Syst.*, vol. 47, no. 7, pp. 1712–1726, Jul. 2017.

[16] Y. Zhou, H. Hu, Y. Liu, and Z. Ding, "A distributed method to avoid higher-order deadlocks in multi-robot systems," *Automatica*, vol. 112, Feb. 2020, Art. no. 108706.

[17] L. E. Kavraki, P. Svestka, J.-C. Latombe, and M. H. Overmars, "Probabilistic roadmaps for path planning in high-dimensional configuration spaces," *IEEE Trans. Robot. Autom.*, vol. 12, no. 4, pp. 566–580, Aug. 1996.

[18] V. R. Desaraju and J. P. How, "Decentralized path planning for multi-agent teams in complex environments using rapidly-exploring random trees," in *Proc. IEEE Int. Conf. Robot. Autom.*, Shanghai, China, May 2011, pp. 4956–4961.

[19] H. Choset, K. M. Lynch, S. Hutchinson, G. A. Kantor, and W. Burgard, *Principles of Robot Motion: Theory, Algorithms, and Implementation*. Boston, MA, USA: MIT Press, 2005.

[20] D. V. Dimarogonas, S. G. Loizou, K. J. Kyriakopoulos, and M. M. Zavlanos, "A feedback stabilization and collision avoidance scheme for multiple independent non-point agents," *Automatica*, vol. 42, no. 2, pp. 229–243, Feb. 2006.

[21] A. K. Pamosoaji and K.-S. Hong, "A path-planning algorithm using vector potential functions in triangular regions," *IEEE Trans. Syst., Man, Cybern., Syst.*, vol. 43, no. 4, pp. 832–842, Jul. 2013.

[22] J. Van den Berg, M. Lin, and D. Manocha, "Reciprocal velocity obstacles for real-time multi-agent navigation," in *Proc. IEEE Int. Conf. Robot. Autom.*, Pasadena, CA, USA, May 2008, pp. 1928–1935.

[23] Y. Chen, M. Cutler, and J. P. How, "Decoupled multiagent path planning via incremental sequential convex programming," in *Proc. IEEE Int. Conf. Robot. Autom.*, Seattle, WA, USA, May 2015, pp. 5954–5961.

[24] Z. Li, J. Deng, R. Lu, Y. Xu, J. Bai, and C.-Y. Su, "Trajectory-tracking control of mobile robot systems incorporating neural-dynamic optimized model predictive approach," *IEEE Trans. Syst., Man, Cybern., Syst.*, vol. 46, no. 6, pp. 740–749, Jun. 2016.

[25] M. Guo and D. V. Dimarogonas, "Multi-agent plan reconfiguration under local LTL specifications," *Int. J. Robot. Res.*, vol. 34, no. 2, pp. 218–235, Feb. 2015.

[26] M. Pivtoraiko, R. A. Knepper, and A. Kelly, "Differentially constrained mobile robot motion planning in state lattices," *J. Field Robot.*, vol. 26, no. 3, pp. 308–333, Mar. 2009.

[27] P. Abichandani, G. Ford, H. Y. Benson, and M. Kam, "Mathematical programming for multi-vehicle motion planning problems," in *Proc. IEEE Int. Conf. Robot. Autom.*, Saint Paul, MN, USA, May 2012, pp. 3315–3322.

[28] M. Jager and B. Nebel, "Decentralized collision avoidance, deadlock detection, and deadlock resolution for multiple mobile robots," in *Proc. IEEE/RSJ Int. Conf. Intell. Robots. Syst.*, vol. 3. Maui, HI, USA, Oct. 2001, pp. 1213–1219.

[29] R. L. Moorthy, W. Hock-Guan, N. Wing-Cheong, and T. Chung-Piaw, "Cyclic deadlock prediction and avoidance for zone-controlled AGV system," *Int. J. Prod. Econ.*, vol. 83, no. 3, pp. 309–324, Mar. 2003.

[30] M. P. Fanti, A. M. Mangini, G. Pedroncelli, and W. Ukovich, "Decentralized deadlock-free control for AGV systems," in *Proc. Amer. Control Conf.*, Chicago, IL, USA, Jul. 2015, pp. 2414–2419.

[31] M. Boukens, A. Boukabou, and M. Chadli, "A real time self-tuning motion controller for mobile robot systems," *IEEE/CAA J. Automatica Sinica*, vol. 6, no. 1, pp. 84–96, Jan. 2019.

[32] Q. Wu, L. Yu, Y.-W. Wang, and W.-A. Zhang, "LESO-based position synchronization control for networked multi-axis servo systems with time-varying delay," *IEEE/CAA J. Automatica Sinica*, vol. 7, no. 4, pp. 1116–1123, Jul. 2020.

[33] T. Wang, X. Xu, and X. Tang, "Scalable clock synchronization analysis: A symmetric noncooperative output feedback tubes-MPC approach," *IEEE/CAA J. Automatica Sinica*, vol. 7, no. 6, pp. 1604–1626, Nov. 2020.

[34] Y. Zhou, H. Hu, Y. Liu, S.-W. Lin, and Z. Ding, "A distributed approach to robust control of multi-robot systems," *Automatica*, vol. 98, pp. 1–13, Dec. 2018.

[35] J. L. Garriga and M. Soroush, "Model predictive control tuning methods: A review," *Ind. Eng. Chem. Res.*, vol. 49, no. 8, pp. 3505–3515, Mar. 2010.

[36] M. Mehndiratta, E. Camci, and E. Kayacan, "Automated tuning of nonlinear model predictive controller by reinforcement learning," in *Proc. IEEE/RSJ Int. Conf. Intell. Robot. Syst.*, Madrid, Spain, Oct. 2018, pp. 3016–3021.

[37] R. Nebeluk and M. Ławryńczuk, "Tuning of multivariable model predictive control for industrial tasks," *Algorithms*, vol. 14, no. 1, p. 10, Jan. 2021.

[38] D. Morgan, S.-J. Chung, and F. Y. Hadaegh, "Model predictive control of swarms of spacecraft using sequential convex programming," *J. Guid. Control Dyn.*, vol. 37, no. 6, pp. 1725–1740, Nov. 2014.

[39] L. Vandenberghe, "Convex optimization: Modeling and algorithms," presented at the 21st Mach. Learn. Summer School, 2012. [Online]. Available: http://www.seas.ucla.edu/ vandenbe/shortcourses/mlss12-convexopt.pdf

[40] P. Jogalekar and M. Woodside, "Evaluating the scalability of distributed systems," *IEEE Trans. Parallel Distrib. Syst.*, vol. 11, no. 6, pp. 589–603, Jun. 2000.

[41] Q. T. Dinh and M. Diehl, "Local convergence of sequential convex programming for nonconvex optimization," in *Recent Advances in Optimization and Its Applications in Engineering*, M. Diehl, F. Glineur, E. Jarlebring, and W. Michiels, Eds. Berlin, Germany: Springer, 2010, pp. 93–102.

[42] H. Zhao, Y. Wen, S. Wu, and J. Deng, "Dynamic evaluation strategies for multiple aircrafts formation using collision and matching probabilities," *IEEE/CAA J. Automatica Sinica*, vol. 8, no. 4, pp. 890–904, Apr. 2021.

[43] T. Zhang, J. Xiao, L. Li, C. Wang, and G. Xie, "Toward coordination control of multiple fish-like robots: Real-time vision-based pose estimation and tracking via deep neural networks," *IEEE/CAA J. Automatica Sinica*, vol. 8, no. 12, pp. 1964–1976, Dec. 2021.

Yuan Zhou (Member, IEEE) received the M.S. degree in computational mathematics from Zhejiang Sci-Tech University, Hangzhou, China, in March 2015, and the Ph.D. degree in computer science from Nanyang Technological University, Singapore, in June 2019.

He is currently a Research Fellow with the School of Computer Science and Engineering, Nanyang Technological University. He has published about 40 research papers in various journals and conferences, including IEEE TRANSACTIONS ON SYSTEMS, MAN, AND CYBERNETICS: SYSTEMS, IEEE TRANSACTIONS ON FUZZY SYSTEMS, IEEE TRANSACTIONS ON SOFTWARE ENGINEERING, IEEE TRANSACTIONS ON AUTOMATION SCIENCE AND ENGINEERING, IEEE TRANSACTIONS ON RELIABILITY, IEEE Symposium on Security and Privacy, International Conference on Robotics and Automation, International Symposium on Software Testing and Analysis, and International Conference on Software Engineering. His research interests focus on the safety and security of autonomous unmanned systems, including multirobot systems and autonomous vehicles.

Hesuan Hu (Senior Member, IEEE) received the B.S. degree in computer engineering and the M.S. and Ph.D. degrees in electromechanical engineering from Xidian University, Xi'an, China, in 2003, 2005, and 2010, respectively.

He is currently a Professor with Xidian University, also a Collaborator with Nanyang Technological University, Singapore, and a Researcher with Xi'an Jiaotong University, Xi'an. His current research interests include discrete-event systems and their supervisory control techniques, Petri nets, automated manufacturing systems, multimedia streaming systems, autonomous vehicles, cyber security, and artificial intelligence. He has over 170 publications in journals, book chapters, and conference proceedings in the above areas. As well, he is a holder of over 40 issued and filed patents in his fields of expertise.

Prof. Hu was a recipient of many national and international awards, including the Franklin V. Taylor Memorial Award for the Best Paper from the IEEE SMC Society in 2010 and the finalists of the Best Automation Paper from the IEEE ICRA Society in 2013, 2016, and 2017. He has been an Associate Editor of the *IEEE Control Systems Magazine*, the *IEEE Robotics & Automation Magazine*, the IEEE TRANSACTIONS ON AUTOMATION SCIENCE AND ENGINEERING, the *IEEE Robotics & Automation Letters*, and the *Journal of Intelligent Manufacturing*. He is an IEEE Distinguished Lecturer.

Gelei Deng received the bachelor's degree in electrical engineering from the Singapore University of Technology and Design, Singapore, in 2018. He is currently pursuing the Ph.D. degree with Nanyang Technological University, Singapore.

His research focuses on computer system security, robotic security, and security testing.

Kun Cheng received the B.S. and Ph.D. degrees in computer science and engineering from the School of Computer Science and Engineering, Beihang University, Beijing, China, in 2012 and 2020, respectively.

His research interests include system virtualization, cloud computing, and safety-critical systems.

Shang-Wei Lin received the B.S. degree in information management and the Ph.D. degree in computer science and information engineering from National Chung Cheng University, Chiayi, Taiwan, in 2003 and 2010, respectively.

He is currently an Assistant Professor with the School of Computer Science and Engineering, Nanyang Technological University, Singapore. His research interests include formal methods, embedded systems, and cyber–physical systems.

Yang Liu (Senior Member, IEEE) received the bachelor's and Ph.D. degrees in computer science from the National University of Singapore (NUS), Singapore, in 2005 and 2010, respectively.

He was a Postdoctoral Fellow with NUS. He is currently a Full Professor with the School of Computer Science and Engineering, Nanyang Technological University, Singapore. His research focuses on software engineering, security, cyber–physical systems, and formal methods. Particularly, he specializes in software verification using model checking techniques, leading to the development of a state-of-the-art model checker, Process Analysis Toolkit.

Zuohua Ding received the M.S. degree in computer science and the Ph.D. degree in mathematics from the University of South Florida, Tampa, FL, USA, in 1996 and 1998, respectively.

From 1998 to 2001, he was a Senior Software Engineer with Advanced Fiber Communication, Petaluma, CA, USA. He has been a Research Professor with the National Institute for Systems Test and Productivity, Vail, CO, USA, since 2001. He is currently a Professor and the Director of the Laboratory of Intelligent Computing and Software Engineering, Zhejiang Sci-Tech University, Hangzhou, China. He has authored and coauthored over 120 papers. His current research interests include system modeling, program analysis, service computing, software reliability prediction, and Petri nets.